SANDIA REPORT
SAND2006-4989
Unlimited Release
Printed August 2006

Design and Performace of a 30 KV Electron Gun with Ten Independent Cathodes and a Magnetic Lens

Kim W. Reed and Joseph M. Rudys

Prepared by
Sandia National Laboratories
Albuquerque, New Mexico 87185 and Livermore, California 94550

Sandia is a multiprogram laboratory operated by Sandia Corporation,
a Lockheed Martin Company, for the United States Department of Energy's
National Nuclear Security Administration under Contract DE-AC04-94AL85000.

Approved for public release; further dissemination unlimited.

DESIGN AND PERFORMANCE OF A 30 KV ELECTRON GUN WITH TEN INDEPENDENT CATHODES & A MAGNETIC LENS

Kim W. Reed and Joseph M. Rudys
Sandia National Laboratories, P.O. Box 580, Mail Stop MS-1152
Albuquerque, New Mexico 87185 USA

Abstract[1]

Measurements on a 30 kV electron gun with ten independent cathodes, operating in a 6.5 Tesla (T) magnetic field are presented. An earlier paper covered the design of this electron gun [1]. Experimental results are compared to model predictions. Beam current is compared to theoretical space charge limited flow.

I. INTRODUCTION

The electron gun accommodates a physics experiment requiring a sheet electron beam to be swept while immersed in an axial 6.5 T static magnetic field. The beam is delivered to the center of a pair of super conducting (SC) solenoidal magnets with axes along the beam, Fig. 1(b). Beam sweeping is affected by sequentially pulsing the elements of a ten-cathode array. Rapid sequential pulsing is achieved by statically charging capacitive stores and electronically pulsing the selected cathode voltages relative to a biased slotted grid – discharging a small portion stored energy per pulse. The 4.6 cm square array of electrons is extracted through a Be foil at the end of a 7.6 cm square x 18.3 cm deep "snout" that penetrates into the magnet center. Fields from the SC magnet focus electrons from the 10 cm square cathode array to the extraction point. Magnet considerations prohibit shielding or magnetic materials in proximity to the electron gun, requiring electronics to be located remotely. Pulse duration and beam current are adjustable. High voltage (HV) insulation is air and vacuum.

II. SYSTEM CONFIGURATION

The electron gun *system* consists of a remotely located (7.6 meter) HV deck, a control console (not shown) and the electron gun, Fig. 1a. The HV deck contains electronics, power supplies, interlocks and energy stores –

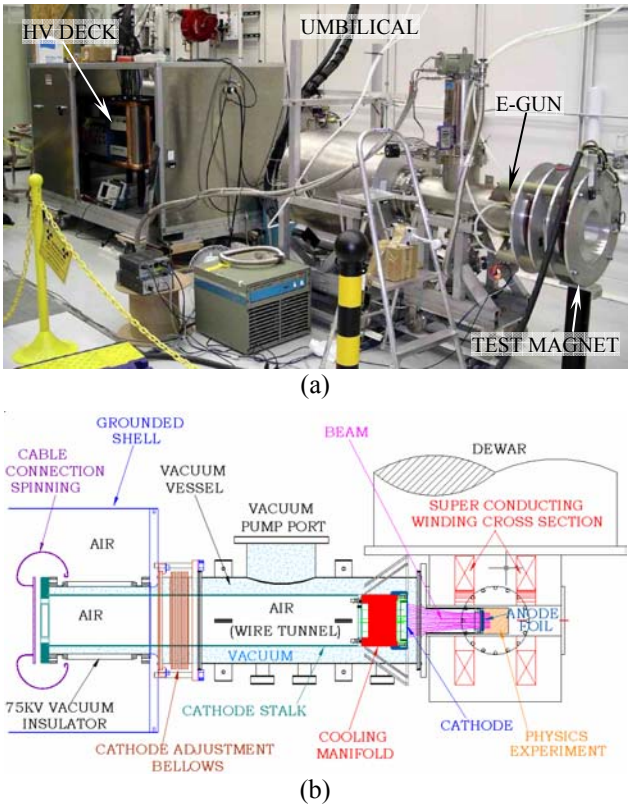

Figure 1. (a) Complete E-Gun system with test magnet. (b) Internal E-Gun elements & SC magnet.

fibreoptically linked to the control console. The electron gun system was commissioned at Sandia prior to shipment to Princeton. A pulsed 0.58 T test magnet that replicates the winding geometry of the Princeton SC magnet provided the same beam focusing as the Princeton magnet during commissioning – TriComp [2] simulations indicate that at 0.58 T the beam envelope will be representative of that at 6.5 T. Energy absorption in the electron window requires an acceleration potential from the cathode stalk to the vacuum vessel of 60 KeV, for a 30 KeV beam energy out of the gun, Fig. 1(b). The system is entirely air insulated except between the cathode stalk and vacuum vessel – shaded light blue in Fig. 1b. Standard practice for microwave devices allows 64KV/cm DC [3] in vacuum, so the electron gun was designed with maximum vacuum stresses of 60KV/cm. Standard practice for high voltage feed-throughs and switches in air allows 5 KV/cm DC [4, 5, 6]. Sea level

[1]Sandia is a multiprogram laboratory operated by Sandia Corporation, a Lockheed Martin Company, for the United States Department of Energy under contract DE-AC04-94AL85000. This work is supported by the NSF in collaboration with Princeton University.

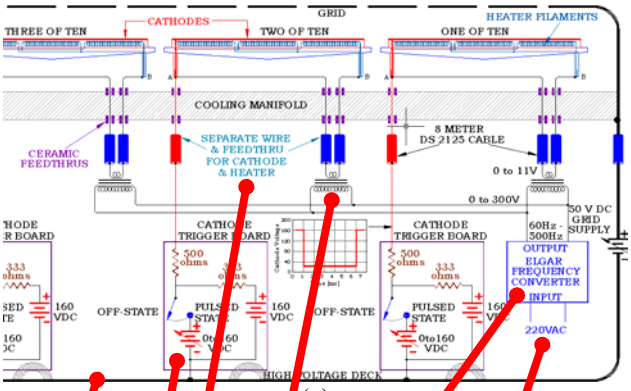

(a)

(b)

Figure 2. (a) HV-deck internal elements.
(b) Electronics cabinet with doors off.

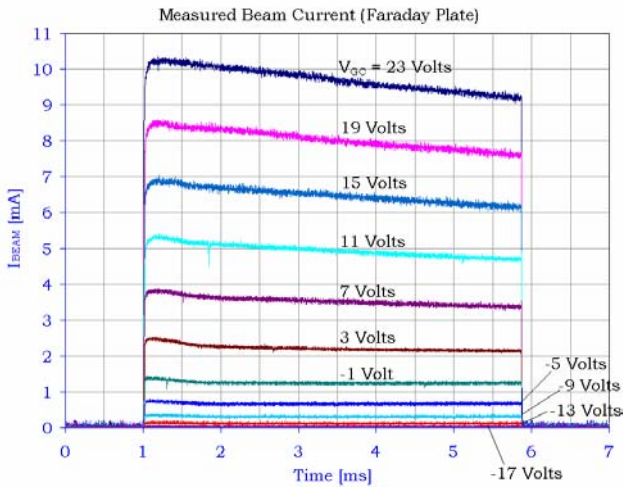

Figure 3. Measured electron current at the anode Faraday plate – inside the vacuum. V_G = 30 Volts

corona leakage rapidly rises at this electrical stress – a function of atmospheric conditions. The design was conservative at 2.6KV/cm in air insulated regions to allow operation over a range of pressure and humidity.

III. MEASUREMENTS

A. Beam Current

Beam currents measured at the anode foil, Fig. 3, have 10%-90% rise and fall times of less than 1μs (not shown) – corresponding to 833Ω driver impedance and 7.6 meters of DS2125 umbilical cable at 103pf/meter – specification is < 40μs. Beam currents flow for negative values of grid-to-cathode voltage (V_{GC}) due to the influence of the HV potential on the grid-cathode region. Higher values of V_{GC} correspond to cathode driver outputs pulsing closer to ground. These currents exhibit fall off with time due to saturation β-loss in the ground referenced transistor that sets the pulsed cathode voltage. Current droop was eliminated by increasing the grid voltage (V_G) from 30 Volts (Fig. 3.) to 50 Volts (Fig. 2a), replicating beam currents at higher pulsed cathode voltages (V_C).

B. Beam Image & Image Rotation

The Faraday plate was replaced by the beam window foil and scintillator (Xerox transparency) photographs were taken of the beam entering the room, Fig. 4.

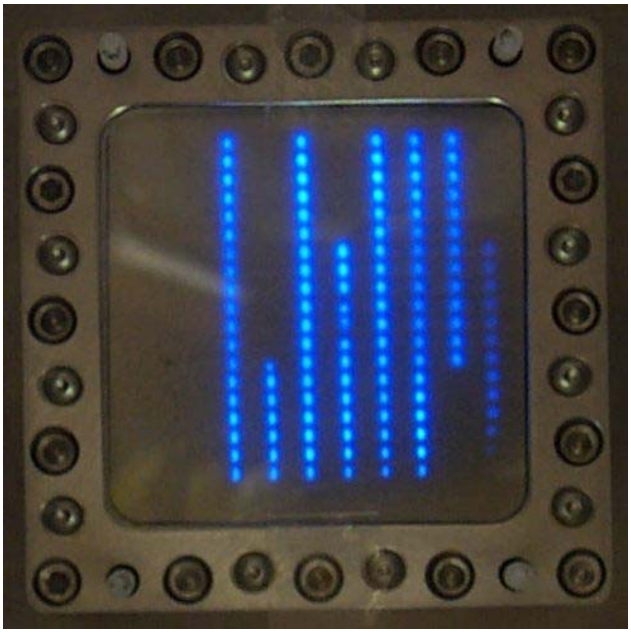

Figure 4. Electron beam exiting the foil (0.58 T magnet).

All components were aligned with gravity, but it was necessary to rotate the snout about 2° CCW relative to the grid slots in the camera view to allow the beam to emerge from the hibachi. Measurement accuracy is that of a string and a plumb-bob. The drift velocities causing this image rotation are,

$$\mathbf{v}_{gradB} = (W_{\perp}/q)\,[\mathbf{B} \times \mathrm{grad}\mathbf{B}]/B^3$$

$$\mathbf{v}_{curvB} = (2W_{\parallel}/q)\,[\mathbf{R}_c \times \mathbf{B}]/(R_c^2 B^2) \qquad (1)$$

$$\mathbf{v}_{ExB} = [\mathbf{E} \times \mathbf{B}]/B^2$$

$W_\perp$ and $W_\parallel$ are particle energy [Joules] perpendicular and parallel to the B-Field, q is signed charge [$\pm$ coulombs] and $\mathbf{R}_c$ is the radius of curvature [meters].

Image rotation (camera view) is due to CW **E**x**B** and CCW curvature drift in the focusing B-Field, Fig. 5.

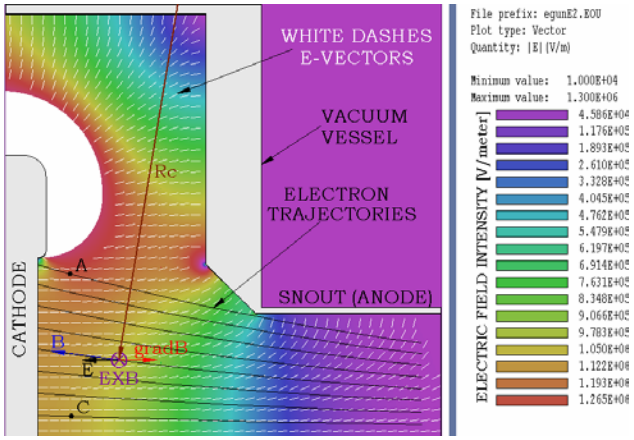

Figure 5. The electric field is concentrated between the cathode and the snout entrance (TriComp).

To minimize electron *momentum-perpendicular* to the B-Field ("beta-perp"), the cathode is designed so that the E-Field launches electrons in a direction "close" to that of the B-Field, $W_\perp \cong 0$ (kT/q is negligible at 1000°C). TriComp simulations indicate that at 0.58 T, Larmor gyrations are barely visible on the beam scale – *a requirement for the test magnet*. This means that the electron orbits sample only a small part of the B-Field yielding very little force imbalance due to grad**B** on opposite sides of the orbits and it confirms that $2W_\parallel >> W_\perp$. Additionally, the small diameter of the beam relative to that of the magnet coils makes grad**B** almost entirely z-directed – very little variation occurs in a plane normal to **B**. The result is that **B** x grad**B** is very small, so gradient drift is not a factor in image rotation. Conversely, inertial forces are large since most of the 60KeV is imparted to the electrons in the small gap between the cathode and the entrance to the snout. The electrons are moving at close to 60KeV where there is still significant curvature in the B-Field. Comparison of **E**x**B** and curvature terms,

$$\begin{aligned} 2W_\parallel/q &\cong -0.120 \text{ MeV} \\ 1/R_c &\cong 1 \text{ meter}^{-1} \\ E &\cong 1.0M \text{ V/meter} \\ |\mathbf{R}_c \times \mathbf{B}| &= R_c B \\ |\mathbf{E} \times \mathbf{B}| &\cong EB/4 \end{aligned} \qquad (2)$$

shows that the two drift components are comparable in magnitude and in *opposite* directions. A TriComp analysis viewed from the camera toward the snout predicts a net CCW rotation of 1.6°, Fig. 6. Most electrons experience similar E & B histories in the critical region before the snout entrance, Fig. 5, so there is very little distortion. TriComp predicts a slight rotation reversal at the cathode

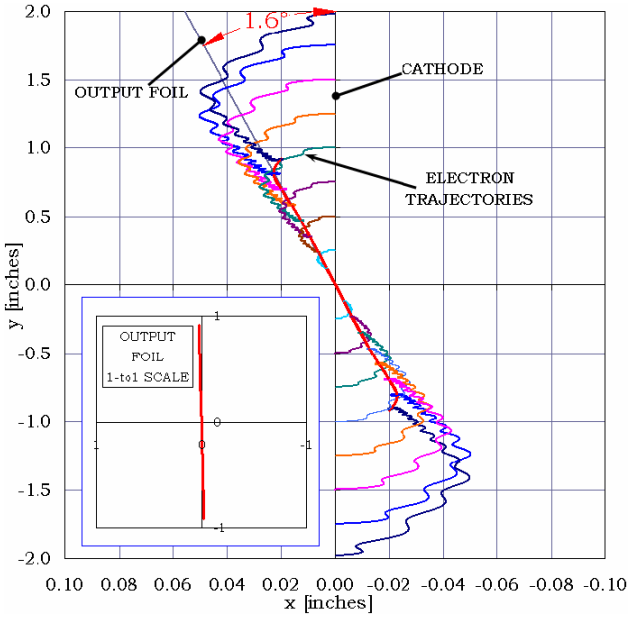

Figure 6. TriComp predicts the "2°" snout rotation

tips - probably due to enhanced **E**x**B** where these electrons pass through the elevated E-Field from the grid clamp, Fig. 5 (Point A). All drift components in Eqn. (1) are inversely proportional to B, making it unnecessary to rotate the cathode relative to the hibachi with 6.5 T.

C. 1-D Space-Charge Limited Flow (SCLF)

The emitted current density for a triode is [7],

$$J = G[V_{GC} + V_{AC}/\mu]^{3/2} \qquad [A/cm^2] \qquad (3)$$

where,

G = perveance (geometry) [$mA/cm^2\text{-volts}^{3/2}$]
V_{GC} = grid to cathode voltage [volts]
V_{AC} = anode to cathode voltage [volts]
μ = a dimensionless constant for the effect of the acceleration field on grid-cathode fields

The cathodes are finite in width and length and are immersed in substantial E-Field perturbations due to the slotted grid. One would expect that a 3-D SCLF model would be required to calculate perveance. However, the strong axial B-Field constrains the electrons to the 1-D case and the perveance is [7],

$$G = 3.16\text{x}10^4(4/9)\varepsilon_o(2e/m_e)^{1/2}/d^2 \quad [mA/cm^2\text{-volts}^{3/2}] \qquad (4)$$

where,
ε_o = permittivity of vacuum [Fd/meter]
e = electronic charge [Coul]
m_e = electronic mass [gm]
d = cathode-grid spacing [cm]

Micrometer measurements obtained d = 0.353 cm at room temperature, so $G_{25°C} = 0.0187$ $mA/cm^2\text{-volts}^{3/2}$, yielding the blue tube characteristic, Fig. 7. d and μ were adjusted to optimally match the data (GREEN DOTS, Fig. 7) to the 1-D space-charge flow theory (RED CURVE, Fig. 7), yielding $G_{1000°C} = 0.0238$ $mA/cm^2\text{-volts}^{3/2}$, $\mu = 1740$ and

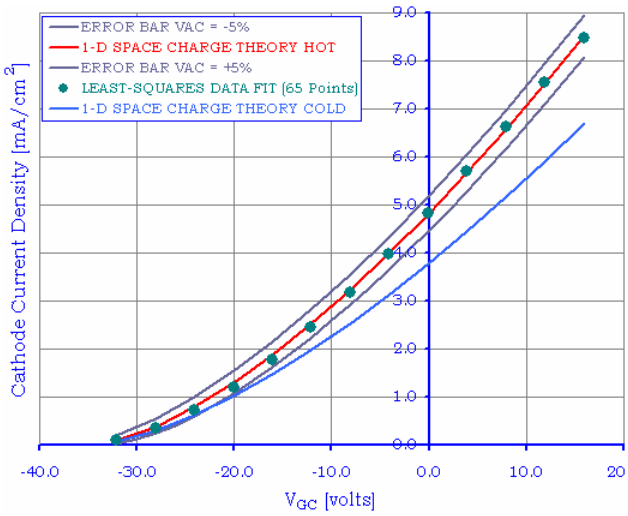

Figure 7. Comparison of measured currents to SCLF.

a value of d 15 mils (~4%) less than was measured at 25°C. This reduction in d could be accounted for by thermal expansion in the stalks that the cathodes are mounted on (cathode operating temperature is 1000°C), slight thermal grid warp (although the grid was mounted with slotted screw holes so that it could float and stay flat as it expanded), measurement error (micrometer tilt) and assembly variations (d was measured at only a couple of places). Another source of error is in the conversion of current in the Faraday plate to current density – requiring a measurement of the beam cross section in the vacuum (not shown here) and an assumption of the current distribution in the beam. The gray error bars represent an uncertainty of ±5% in the acceleration potential, V_{AC}. In this comparison, beam current attenuation in the foil was accounted for using CYLTRAN [8].

IV. CONCLUSIONS

This electron gun called for independently adjustable current densities in the extracted beam of 0 to 5 mA/cm^2. With V_G = 50 volts, this current density range corresponds to 50 volts<V_C< 82 volts – well away from the point that transistors saturate on the trigger board – yielding constant current pulses for the required 5 ms duration. Pulse length can be varied from 0 to 5 ms by controlling the pulse generator that triggers the gun (requires 50Ω, TTL). Beam voltage was specified at 30 KeV out of the foil. CYLTRAN analysis indicates that the peak extracted beam energy is 33 KeV with the internal acceleration potential set at 60 KeV [1].

V. REFERENCES

[1] K.W. Reed, G.E. Pena, L.X. Schneider & J. M. Rudys, "A Novel Electron Gun with an Independently Addressable Cathode Array," Proc. IEEE Pulsed Power Plasma Science 2001, 01CH37251, 2001, pp. 126-129.

[2] TriComp for Windows, Field Precision, P.O. Box 13595, Albuquerque, NM, (505) 220-3975 http://techinfo@fieldp.com

[3] "The Handbook of Microwave Technology", Vol. 1, 1995 in Plastics, Vol. 3, particularly note the reference made to Armand Straprans at Varian cited on pg. 538.

[4] "Products for High-Voltage Insulated Devices" Product Catalog, Isolation Products, Inc., 157 SanLazaro, Sunnyvale, CA 94086, (408) 730-4672.

[5] "High Voltage Relays", Product Catalog, Ross Engineering Corp., 540 Westchester Dr., Campbell, CA 95008, (408) 377-4621.

[6] Measurements at Sandia National Laboratories.

[7] W.W. Harmon, "Fundamentals of Electronic Motion", NY: McGraw-Hill, 1953, Lib of Cong. 52-13456, Ch 5.

[8] J.A. Halbleib, R.P Kensek, et al, "ITS Version 3.0: The Integrated TIGER Series of Coupled Electron/Photon Monte Carlo Transport Codes," SAND Doc: SAND91-1634•UC-405, March 1992.

APPENDIX A

A. Lessons Learned- Dispenser Cathodes

- Use separate heater & cathode wires/cables except right at the cathode (see Fig. 2a) – otherwise the high AC heater current can modulate the cathode voltage.
- Heater must be AC with one end connected to cathode.
- Protect electronics in a Faraday cage with MOVs, spark-gaps & capacitors. Connect spark gaps so they won't stay lit after fault passes.
- Heat cathodes slowly after air exposure to prevent cathode plate out – watch vacuum when conditioning.
- Choose materials exposed to heat that don't react with cathode oxides, especially the grid – molybdenum is good, but Al and S bearing compounds are bad.
- Mount grid so that it can expand without warping.
- Actively cool the grid if possible.
- Vacuum should be low 10^{-8} Torr for long cathode life.
- Cooling barrier should block conduction/radiation from cathodes to temperature sensitive materials – everything in cathode line-of-site will get hot.
- Thermally isolate cathodes on stalks to allow efficient heating – cool the base of the stalks if possible.
- Correlate cathode temperature to input power *in-situ* – temperature depends upon mounting and surroundings.
- Compartment the cathodes to prevent interaction.
- Avoid insulator line-of-site to cathode – plating issues.
- Prefer Conflat seals – won't outgas & allow bake-out.
- Secure the cathode elements & exposed filament wires in ceramics so that they can't move/short when heated.
- Once heated, brittle filament wires cannot be moved.
- Vacuum insulation requires good HV conditioning.
- Remove HV energy stores during HV conditioning.
- Pulse grid if possible – only has displacement currents.

Issued by Sandia National Laboratories, operated for the United States Department of Energy by Sandia Corporation.

NOTICE: This report was prepared as an account of work sponsored by an agency of the United States Government. Neither the United States Government, nor any agency thereof, nor any of their employees, nor any of their contractors, subcontractors, or their employees, make any warranty, express or implied, or assume any legal liability or responsibility for the accuracy, completeness, or usefulness of any information, apparatus, product, or process disclosed, or represent that its use would not infringe privately owned rights. Reference herein to any specific commercial product, process, or service by trade name, trademark, manufacturer, or otherwise, does not necessarily constitute or imply its endorsement, recommendation, or favoring by the United States Government, any agency thereof, or any of their contractors or subcontractors. The views and opinions expressed herein do not necessarily state or reflect those of the United States Government, any agency thereof, or any of their contractors.

Printed in the United States of America. This report has been reproduced directly from the best available copy.

Available to DOE and DOE contractors from
U.S. Department of Energy
Office of Scientific and Technical Information
P.O. Box 62
Oak Ridge, TN 37831

Telephone: (865) 576-8401
Facsimile: (865) 576-5728
E-Mail: reports@adonis.osti.gov
Online ordering: http://www.osti.gov/bridge

Available to the public from
U.S. Department of Commerce
National Technical Information Service
5285 Port Royal Rd.
Springfield, VA 22161

Telephone: (800) 553-6847
Facsimile: (703) 605-6900
E-Mail: orders@ntis.fedworld.gov
Online order: http://www.ntis.gov/help/ordermethods.asp?loc=7-4-0#online

Distribution List:

1	MS 1152	Marilyn Bange, 1654
1	MS 1152	Steve Glover, 1654
1	MS 1152	Gary Pena, 1654
1	MS 1152	Kim Reed, 1654
1	MS 1182	Bob Turman, 1654
1	MS 1182	Ron Kaye, 5445
1	MS 1182	Tom Lockner, 5445
1	MS 1181	Larry Schneider, 1650
2	MS 0899	Tech Library, 4536
2	MS 9018	Central Tech Files, 8944

Sandia National Laboratories